Dynamic Interface Crack Propagating Along a Line Between Two Holes

Ouk Sub Lee*, Jae Chul Park, Hai Long Yin, Kwi Hwan Byun
School of Mechanical, Aerospace and Automation Engineering, Inha University

The effects of the interface and two holes located near the crack path in the hybrid specimen on the dynamic crack propagation behavior have been investigated using dynamic photoelasticity with the aid of Cranz-Shardin type high speed camera system. The dynamic stress field around the dynamically propagating interface crack tip in the three point bending specimens under a dynamic load applied by a hammer dropped from 0.6 m high without initial velocity are recorded. The complex stress intensity factors for the dynamically propagating interface crack are extracted by using a overdeterministic least square method. Theoretical dynamic interface isochromatic fringe loops generated by using the numerically determined complex stress intensity factors are compared with the experimental results. Furthermore, the influence of the hole to the dynamic interface crack velocities has been investigated experimentally.

Key Words : Dynamic Interface Crack, Rayleigh Wave, Dynamic Crack Propagating Velocity, Dynamic Isochromatic Fringe Loops, Dynamic Stress Intensity Factor, Two Holes

1. Introduction

During the last few decades many interesting problems pertaining to dynamic crack propagation and arrest phenomena have been investigated by many researchers throughout the world (Dally 1979, Durelli & Dally 1975, Freund 1976, Kobayashi 1978, Lee & Hong 1996, Lee et al. 1996, Lee & Kim 1999, Singh & Shukla 1996a, b). In recent years, there has been considerable interest in the study of dynamic bimaterial interface crack propagation from both theoretical, numerical and experimental viewpoints since joint structures have been widely used in aerospace, automobile, and electronic fields. (Anderson 1977, Comninou 1990, Deng 1992, Deng 1993, Rice et al. 1965, Wang et al. 1998, Williams 1959, Xu & Needleman 1996, Yang et al. 1991). Even though the majority of these studies have been either analytical or numerical in nature, a few experimental studies on the dynamic interfacial fracture have been appeared in the Technical Journals from 1991. Rosakis group at California Institute of Technology and Shukla group at University of Rhode Island are the representatives among others.

In this study, we have attempted to experimentally investigate the effects of two holes located near the dynamically propagating interface crack path on the crack propagation behavior using the dynamic photoelasticity. The initial failure was obtained by subjecting the bimaterial three point bend specimen to mode I impact loading. The dynamic isochromatic fringe patterns surrounding a crack tip propagating along a bimaterial interface are photographed and characterized. The primary relevant fracture parameters such as the complex stress intensity factors, K_1 and K_2, for the stress field surrounding the dynamic interface crack tip are extracted by using a hybrid experi-

* Corresponding Author,
E-mail : leeos@dragon.inha.ac.kr
TEL : +82-32-860-7315 ; **FAX** : +82-32-868-1716
School of Mechanical, Aerospace and Automation Engineering, Inha University, Inchon 402-751, Korea.
(Manuscript **Received** April 24, 2000; **Revised** November 10, 2000)

mental-theoretical technique.

2. Theoretical

2.1 Stress field and dynamic stress intensity factors at the dynamic interface crack tip

The stress field shown in Fig. 1 at the dynamic interface crack tip developed by Deng (Deng 1993) are rearranged to fit the photoelastic analysis conducted in this study as below in polar coordinate system.

$$\sigma_{xx}(r,\theta)=\frac{1}{\sqrt{2\pi r}}[K_1\cos(\varepsilon\ln r)-K_2\sin(\varepsilon\ln r)]\hat{\sigma}^{I}_{xx0}(\theta)$$
$$+\frac{1}{\sqrt{2\pi r}}\eta[K_1\sin(\varepsilon\ln r)+K_2\cos(\varepsilon\ln r)]\hat{\sigma}^{II}_{xx0}(\theta)$$
$$+\frac{1}{\sqrt{2\pi r}}K_3\hat{\sigma}^{III}_{xx0}(\theta)+\textit{Higher Order Terms} \quad (1)$$

$$\sigma_{yy}(r,\theta)=\frac{1}{\sqrt{2\pi r}}[K_1\cos(\varepsilon\ln r)-K_2\sin(\varepsilon\ln r)]\hat{\sigma}^{I}_{yy0}(\theta)$$
$$+\frac{1}{\sqrt{2\pi r}}\eta[K_1\sin(\varepsilon\ln r)+K_2\cos(\varepsilon\ln r)]\hat{\sigma}^{II}_{yy0}(\theta)$$
$$+\frac{1}{\sqrt{2\pi r}}K_3\hat{\sigma}^{III}_{yy0}(\theta)+\textit{Higher Order Terms} \quad (2)$$

$$\sigma_{xy}(r,\theta)=\frac{1}{\sqrt{2\pi r}}[K_1\cos(\varepsilon\ln r)-K_2\sin(\varepsilon\ln r)]\hat{\sigma}^{I}_{xy0}(\theta)$$
$$+\frac{1}{\sqrt{2\pi r}}\eta[K_1\sin(\varepsilon\ln r)+K_2\cos(\varepsilon\ln r)]\hat{\sigma}^{II}_{xy0}(\theta)$$
$$+\frac{1}{\sqrt{2\pi r}}K_3\hat{\sigma}^{III}_{xy0}(\theta)+\textit{Higher Order Terms} \quad (3)$$

The contants and meaning of the sign appeared in Eqs. (1), (2) and (3) should be refered in a paper by Lee et al. (Lee & Kobayashi 2000, Lee & Park 2000). Combining the stress-optics law (Dally & Riley 1991) with $\tau_m=Nf_\sigma/2t$, we may relate the experimental results with the theoretical stress field as below.

$$\left(\frac{Nf_\sigma}{t}\right)^2=(2\tau_m)^2=(\sigma_{xx}-\sigma_{yy})^2+(2\sigma_{xy})^2$$

where N is the experimental fringe order of the dynamic isochromatic pattern,
f_σ is the dynamic fringe constant of the photoelastic material (6.7 *kN/m-fringe* for polycarbonate),
t is the specimen thickness.

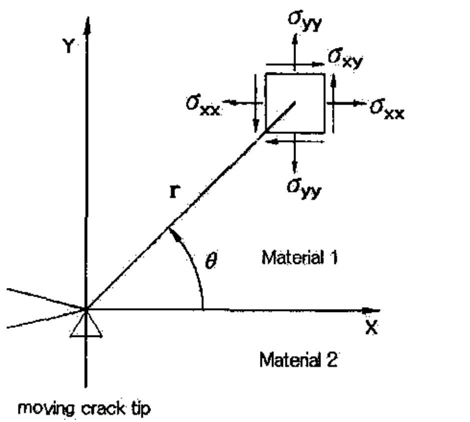

Fig. 1 A coordinate system and stress component for a small element at the dynamic interface crack tip

3. Experimental

3.1 *Multi-spark camera system*

The dynamic photoelasticity method consists of the Cranz-Shardin camera system with a multi-spark camera set, a photoelastic apparatus, a loading equipment, field lens and controllers as shown in Fig. 2. A general view of the experimental setup is shown in Fig. 3.

The spark time delay can be controlled by using the start delay and horizontal・vertical delay in the range from 1 μsec to 0.1sec for each frame. The pulse time to high speed camera frame is measured by using optical detecter to check the reliability of the framing rate.

3.2 Specimen and loading

Revealing the dynamic interface crack propaga-

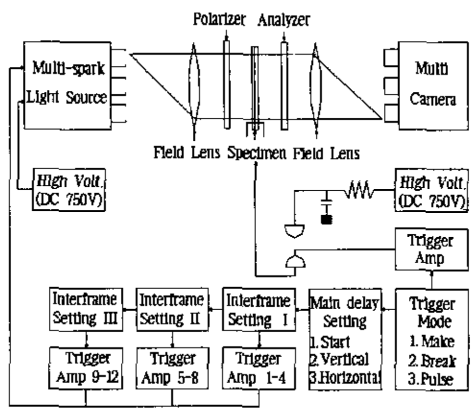

Fig. 2 Block diagram of photoelasticity experimental setup

Table 1 Material and physical properties of Polycarbonate and Aluminum

Properties \ Materials	Polycarbonate	Aluminum
Young's modulus, E(GPa)	2.72	71.0
Poisson's ratio	0.38	0.33
Shear modulus (GPa)	0.98	…
Density (g/cm^3)	1.196	2.80
Material stress-optics fringe value (MPa-mm/fr)	6.7	…
Dilatational wave speed (m/s)	1960	6320
Distortional wave speed (m/s)	910	3100

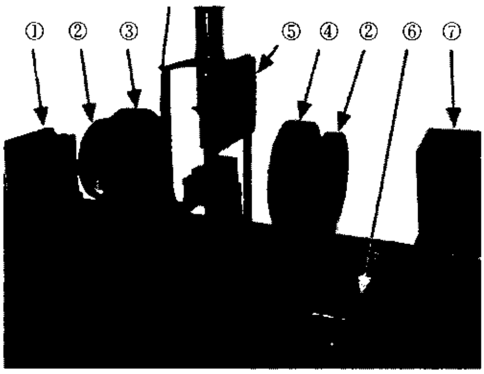

1. Camera 2. Field lens 3. Polarizer
4. Analyser 5. Loading apparatus
6. Trigger controller
7. Multi-spark high speed light sourse

Fig. 3 A general view of dynamic photoelasticity experimental setup

tion phenomena and the dynamic stress field surrounding the dynamic interface crack propagating along a path near two holes, composite specimens with and without two holes are prepared using polycarbonate(PC) and aluminum(Al) as shown in Fig. 4. After we clean up the interface of PC and Al, the halves are bonded together by epoxy and utilizer with a ratio of 1:1. The thickness of the interface should be kept as about 0.09～0.1mm. The residual stress along the interface is measured to be negligible by using a photoelasticity setup. The specimen thick-

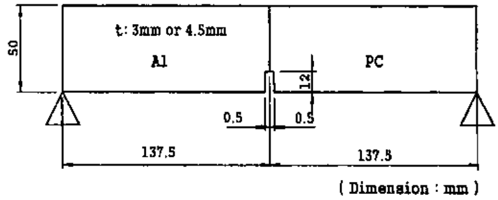

Fig. 4(a) Configuration of test specimen without holes

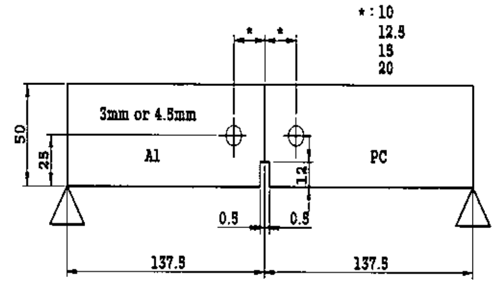

Fig. 4(b) Configuration of test specimen with holes

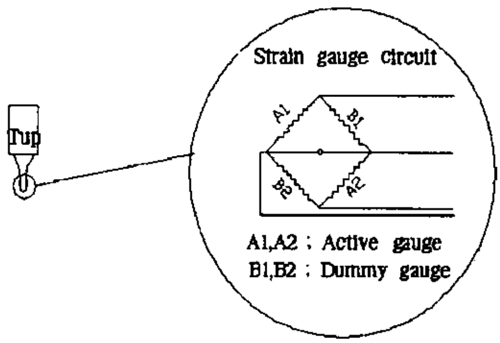

Fig. 5 Configuration of strain gauge circuit attached on impact tup

nesses are 3mm and 4.5mm. We use an electric signal activated at the moment when the impact tup contacts the lead wire on the specimen to trigger the dynamic-experimental system. The impact tup (44Newton) was designed to be free dropped vertically from a height of 80 mm. The trace of dynamic load activated by the impact tup was measured by using the Wheatstone circuit composed of strain gages attached on the tup shown in Fig. 5.

The mechanical and physical properties of PC and Al-7075 are listed in Table 1. Figure 4 shows specimen configurations with and without holes.

4. Results and Consideration

The impact load trace vs. time is shown in Fig. 6. The arrows indicates the crack initiation. It is interesting to note that the crack needs the incubation time of about 140 μsec. And the crack initiation appear to be occurred at the moment far after a load reaches its maximum.

Figures 7 and 8 show the experimentally obtained isochromatic fringe loops at the vicinity of the dynamically propagating interface crack tip in the composite specimens of the thickness 4.5mm and 3mm, respectively. The stress fields have been used to determine the dynamic interface stress intensity factors with the help of the Over-deterministic Least Square(ODLS) methods(Sanford 1980). The extracted interface dynamic complex stress intensity factors have been employed to generate the theoretical fringe loops by using a hybrid experimental-theoretical process. The theoretically generated isochromatics are found to agree well with the experimental isochromatics especially near the crack tip as shown in Figs. 7 and 8. The far fields do not agree each other in two figures since we do not include higher order term in this study.

Figures 9 and 10 shows the variation of the

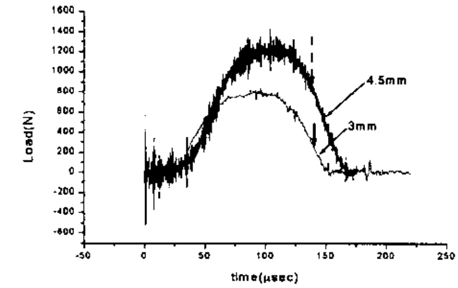

Fig. 6 Load history with respect to time(···→ : crack initiation point for 4.5mm thick specimen ——→ : crack initiation point for 3mm thick specimen)

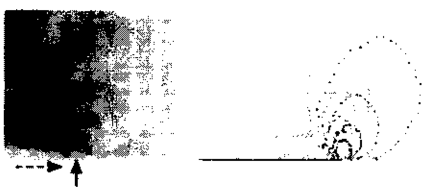

(a) 150 μsec (K_1: 1.4 $MPa\sqrt{m}$, K_2: 1.6 $MPa\sqrt{m}$)

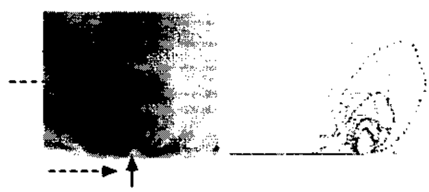

(b) 200 μsec (K_1: 1.5 $MPa\sqrt{m}$, K_2: 1.4 $MPa\sqrt{m}$)

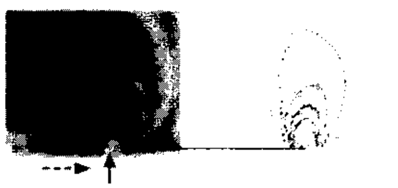

(c) 250 μsec (K_1: 1.9 $MPa\sqrt{m}$, K_2: 0.8 $MPa\sqrt{m}$)

(d) 300 μsec (K_1: 1.9 $MPa\sqrt{m}$, K_2: 0.6 $MPa\sqrt{m}$)

(e) 350 μsec (K_1: 1.7 $MPa\sqrt{m}$, K_2: 1.4 $MPa\sqrt{m}$)

Fig. 7 Experimental and theoretical isochromatic fringe patterns for a crack propagating along the interface (t: 4.5mm) (time is period after impact)
(——→ : instantaneous crack tip position, ···→ : propagating direction)

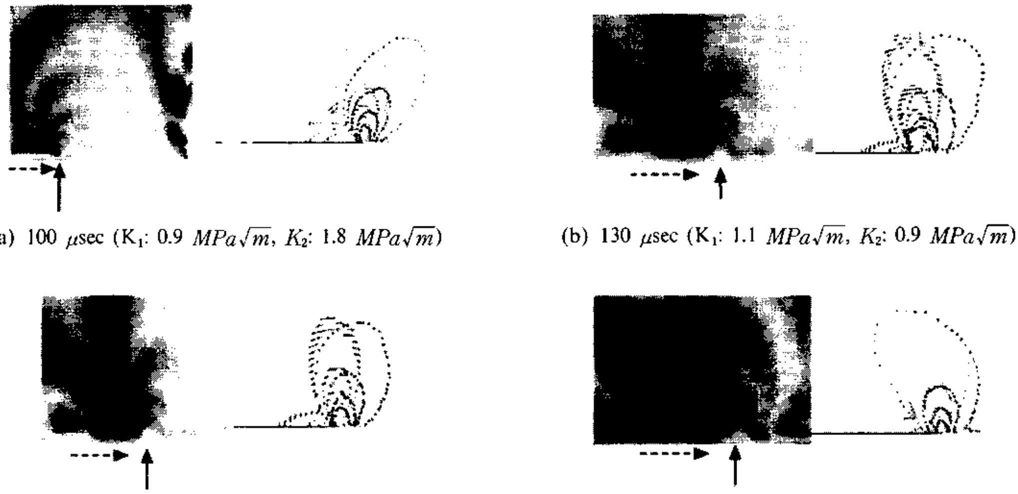

(a) 100 μsec (K_1: 0.9 $MPa\sqrt{m}$, K_2: 1.8 $MPa\sqrt{m}$) (b) 130 μsec (K_1: 1.1 $MPa\sqrt{m}$, K_2: 0.9 $MPa\sqrt{m}$)

(c) 160 μsec (K_1: 1.0 $MPa\sqrt{m}$, K_2: 0.9 $MPa\sqrt{m}$) (d) 201 μsec (K_1: 1.3 $MPa\sqrt{m}$, K_2: 1.2 $MPa\sqrt{m}$)

Fig. 8 Experimental and theoretical isochromatic fringe patterns for a crack propagating along the interface (t: 3mm) (time is period after impact)
(——→ : instantaneous crack tip position, ···→ : propagating direction)

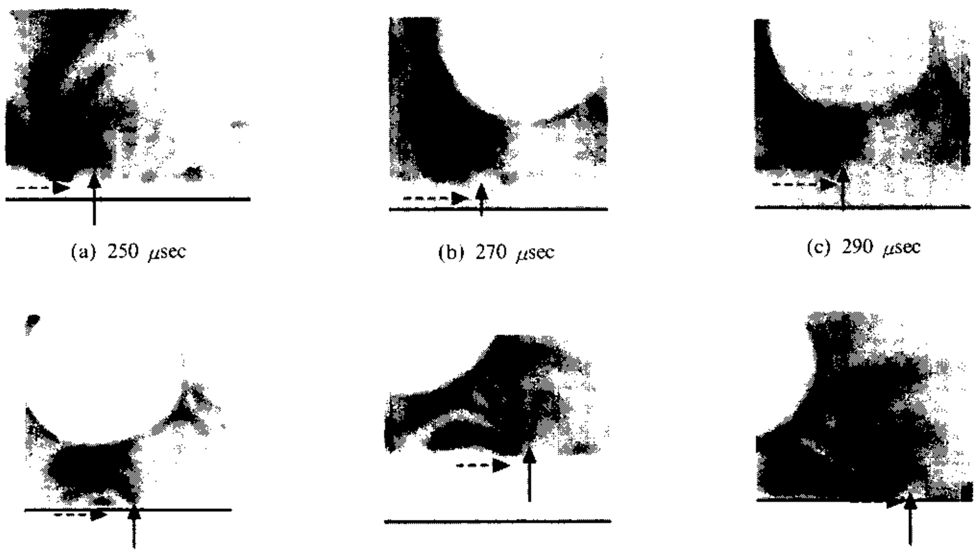

(a) 250 μsec (b) 270 μsec (c) 290 μsec

(d) 310 μsec (e) 330 μsec (f) 350 μsec

Fig. 9 Experimental isochromatic fringe patterns for a crack propagating along the interface with holes centered at 10mm from the interface(t: 4.5mm) (time is period after impact)
(——→ : instantaneous crack tip position, ···→ : propagating direction)

dynamic interface isochromatics and the locations of cracks which propagate along the path between two holes centerd at 10mm and 20mm, from the interface respectively.

Figures 11 and 12 shows relationships between interface stress intensity factors and dynamic crack tip velocities for two different thickness specimens. It is interesting to note from these experimental results that the initial K_1 is quite different from the arrest K_1 and K_2's are the similar for both initiation and arrest phases. The physical meaning of these results should be fur-

(a) 190 μsec

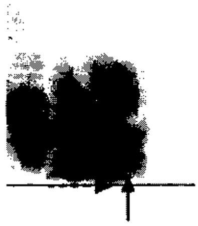

(b) 215 μsec

(c) 240 μsec

(d) 265 μsec

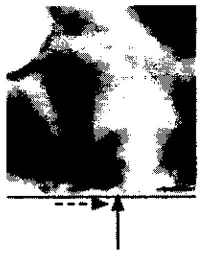

(e) 290 μsec

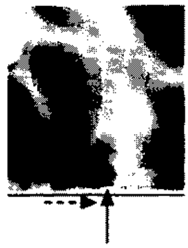

(f) 315 μsec

Fig. 10 Experimental isochromatic fringe patterns for a crack propagating along the interface with holes centered at 10mm from the interface(t: 4.5mm) (time is period after impact) (——→ ; instantaneous crack tip position, ···→ ; propagating direction)

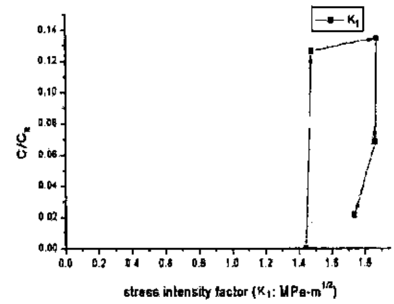

(a) K_1: C/C_R

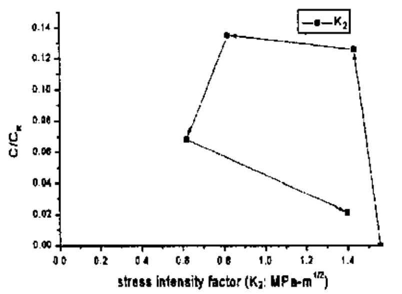

(b) K_2: C/C_R

Fig. 11 Stress intensity factor vs. crack propagating (C/C_R) velocity(t=4.5 mm)

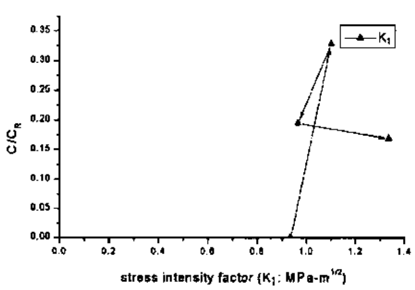

(a) K_1: C/C_R

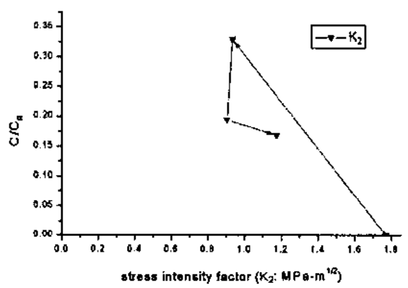

(b) K_2: C/C_R

Fig. 12 Stress intensity factor vs. crack propagating (C/C_R) velocity(t=4.5 mm)

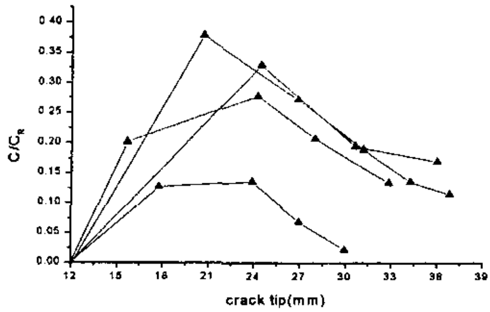

Fig. 13 Crack propagating (C/C_R) velocity vs. Crack tip location

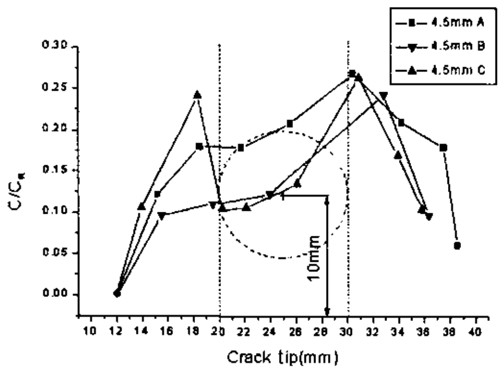

Fig. 14 Crack propagating (C/C_R) velocity vs. crack tip location (specimen having holes centered at 10mm from the interface)

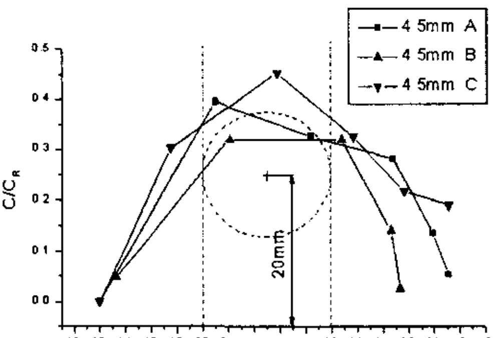

Fig. 15 Crack propagating (C/C_R) velocity vs. crack tip location (specimen having holes centered at 20mm from the interface)

ther investigated.

It is found that the interface dynamic cracks in three point bend specimens propagate with the velocities 15-50% of Rayleigh wave velocity of PC as shown in Fig. 13 and that it is a little bit larger that the velocity in isotropic PC.

The effects of the holes located around the crack propagation path on the crack velocities are shown in Figs. 14 and 15. It is notable that the closer of the 10mm-diameter-hole to the interface, the slower the crack velocities.

5. Concluding Remarks

The interface crack propagation behavior in the three point bend specimen with and without holes under the mode I impact loading condion has been investigated by using the dynamic photoelasticity methods. The results obtained are as follows:

(1) The interface crack velocities are somewhat larger than those in the isotropic PC specimen.

(2) The holes located near the propagation path are found to affect the interface crack propagation speed significantly.

(3) It is noted that the closer the location of 10mm-diameter-hole to the interface, the slower the crack velocities.

(4) It is experimentally observed that the initial and arrest K_1 are quite different in magnitude and arrest K_2 converges to initiation value.

Acknowledgement

This project has been supported by KOSEF special research fund during 1997-2000.

References

Anderson, G. P., et al., 1977, *Analysis and Testing of Adhesive Bond*, Academic Press, New York.

Comninou, M., 1990, "An Overview of Interface Cracks," *Engineering Fracture Mechanics*, Vol. 37, pp. 197~208.

Dally, J. W., 1979, "Dynamic Photoelstic Studies of Fracture," *Experimental Mechanics*, Vol. 19. No. 10, pp. 349~369.

Dally, J. W. and Riley, W. F., 1991, *Experimental Stress Analysis*, McGraw Hill, pp. 424~506.

Deng, X., 1992, "Complete Complex Series Expansions of Near-Tip Fields for Steadily

Growing Interface Cracks in Dissimilar Isotropic Materials," *Engineering Fracture Mechanics*, Vol. 42, No. 2, pp. 237~242.

Deng, X., 1993, "Genaral Crack-Tip Fields for Stationary and Steadily Growing Interface Cracks in Anisotropic Bimaterials," *Journal of Applied Mechanics*, Vol. 60, pp. 183~189.

Durelli, A. J. and Dally, J. W., 1975, "Stress Concentration Factors Under Dynamic Loading Conditions," *Jounal of Mechanical Engineering Science*, Vol. 16. No. 1, pp. 69~92.

Freund, L. B., 1976, "Dynamic Crack Propagation," *Mechanics of Fracture*, Vol. 19, edited by F. Erdogan, ASME, pp. 105~134.

Kobayashi, A. S. and Mall, S., 1978, "Dynamic Fracture Toughness of Homalite-100," *Experimental Mechanics*, Vol. 18, No. 1, pp. 11~18.

Lee, O. S. and Hong, S. K., 1997, "Dynamic Fracture Characteristics of Highly Brittle Materials by Using Instrumented Charpy Impact Test," *KSME International Journal*, Vol. 11, No. 5. pp. 513~520.

Lee, O. S., et al., 1999, "Characteristics of Interface Crack Propagation under Impact Loading"(in Korean), ADD conference.

Lee, O. S. Hwang, S. W. and Nah, K. C., "Analysis of Contact Singular Stresses with Relief Notch by Using Dynamic Photoelsticity (Ⅱ)," (in Korean), *Transaction of the KSME*, Vol. 20, No. 7, pp. 2097~2107.

Lee, O. S. and Kim, D. Y., 1999, "Crack-Arrest Phenomenon of an Aluminum Alloy," *Mechanics Research Communications*, Vol. 26, No. 5, pp. 575~581.

Lee, O. S. and Park, J. C., 2000, "Dynamic mixed mode crack propagation behavior of structural bonded joints," submitted for the publication to *KSME Int. Journal*.

Rice., J. R. and Sih, G. C., 1965, "Plane Problems of Cracks in a Dissimilar Media," *ASME J. Appl. Mech.*, Vol. 32, pp. 418~423.

Sanford, R. J., 1980, "Application of the Least Square Method to the Photoelastic Analysis," *Experimental Mechanics*, Vol. 20, pp. 192~197

Singh, R. P. and Shukla, A, 1996a, "Subsonic and Transonic Crack Growth along a Bimaterial Interface," *International Journal of Fracture*, Vol. 63, pp. 293~310.

Singh, R. P. and Shukla, A., 1996b, "Characterization of Isochromatics Fringe Patterns for a Dynamic Propagating Interface Crack," *International Journal Fracture*, Vol. 76, pp. 293~310.

Wang, W. et al., 1998, "Effect of Elastic Mismatch in Intersonic Crack Propagation Along a Bimaterial Interface," *Engineering Fracture Mechanics*, Vol. 61, pp. 471~485.

Williams, M. L., 1959, "The Stresses Around a Fault or Cracks in Dissimilar Media," *Bulletin of Seismological Society of America*, Vol. 49, No. 2, pp. 199~204.

Xu, X. P. and Needleman, A., 1996, "Numerical Simulations of Dynamic Crack Growth along an Interface," *International Journal of Fracture*, Vol. 74, pp. 289~324.

Yang, W., Suo, Z and Shih, C. F., 1991, "Mechanics of Dynamic Debonding," *Proceedings of Royal Society of London, Series A*, Vol. 433, pp. 679~697.